Large HCO^+ and HCN abundances in the translucent cloud toward PKS 0528+134

Michiel R. Hogerheijde

Sterrewacht Leiden

Eugène J. de Geus

Owens Valley Radio Observatory

Marco Spaans

Sterrewacht Leiden

Huib Jan van Langevelde[1]

Joint Institute for VLBI in Europe

and

Ewine F. van Dishoeck

Sterrewacht Leiden

Received September 13, 1994; accepted ____________

---

[1]currently at NRAO AOC

ABSTRACT

Observations of ^{12}CO J=1–0, ^{13}CO 1–0, HCO$^+$ 1–0, HCN 1–0, and CS 2–1 absorption against the quasar PKS 0528+134 obtained with the Owens Valley Millimeter Array are presented. The line of sight to this standard phase calibrator crosses the diffuse outer edge of the dark cloud B30, located in the λ Ori ring of clouds. Excitation analysis of these absorption lines and ^{12}CO 1–0 emission yields an estimate of the H$_2$ number density of $n_{\rm H_2} = 100 - 500$ cm^{-3}, which is much lower than found toward lines of sight studied previously by millimeter absorption lines. Surprisingly, HCO$^+$ and HCN are found to have abundances relative to ^{12}CO in this diffuse cloud which are comparable to or larger than those found in dark clouds. Significant differences in line width are found between ^{12}CO, HCN and HCO$^+$ which cannot be attributed to line saturation. A possible explanation for the observed abundances and line widths involving cloud turbulence and the chemistry of CH$^+$ is proposed. It is concluded that HCO$^+$ absorption lines sample low density regions which cannot be observed in molecular emission or even in CO absorption.

Subject headings: ISM: abundances, kinematics and dynamics, molecules — line: profiles — molecular processes — turbulence

1. Introduction

Until recently, the amount of information on the chemistry of diffuse and translucent clouds was limited by the low spectral resolution of optical absorption line studies and the usually weak millimeter emission lines of molecules other than CO. The development of millimeter wave interferometers such as that at the Owens Valley Radio Observatory (OVRO) has opened up the possibility for absorption line studies against bright extragalactic millimeter sources, providing high spectral resolution in a wavelength region were many species have strong transitions (Marscher, Bania & Wang 1991; Bania, Marscher & Barvainis 1991; Lucas & Liszt 1994; Lequeux, Allen & Guilloteau 1994; Wilson & Mauersberger 1994; de Geus & Phillips 1995).

Liszt & Wilson (1993) have searched a great number of extragalactic millimeter continuum sources for the presence of Galactic CO J=1–0 emission using single dish telescopes. Lucas & Liszt (1994) present molecular absorption line observations toward three of these sources. Strong, multiple lines of ^{12}CO, ^{13}CO, HCO^+, and HCN are detected. They conclude that the abundances of HCN and HCO^+ with respect to ^{12}CO differ by more than an order of magnitude between different lines of sight, and are surprisingly large in some cases. At radio wavelengths rotational absorption line studies of OH (Crutcher 1980), H_2CO (Colgan, Salpeter & Terzian 1986), and C_3H_2 (Cox, Güsten & Henkel 1988) have been detected in the Taurus dark cloud toward 3C123 and 3C111 indicating large abundances of these molecules. Recently, Liszt & Lucas (1994) reported the detection of weak HCO^+ 1–0 emission from the diffuse cloud toward ζ Oph.

In this Letter, we present observations of absorption lines of ^{12}CO 1–0 and 2–1, HCO^+ 1–0, and HCN 1–0, and upper limits on ^{13}CO 1–0 and CS 2–1, against the quasar PKS 0528+134 obtained from the OVRO database (Scoville et al. 1993). This line of sight crosses the diffuse outer edge of the dark cloud B30 which will be shown to be less dense, and probably warmer than lines of sight studied so far. It provides a unique opportunity to probe the chemistry and physics of such a different environment. In particular, a new explanation for the large abundances and the line widths is proposed which involves CH^+, a species which is known to be abundant in diffuse clouds from optical absorption line observations (Gredel, van Dishoeck & Black 1993; Crawford et al. 1994), but whose role in the chemistry of other species has not yet been recognized.

2. Observations

The quasar PKS 0528+134 ($\alpha_{1950.0} = 05^{\rm h}28^{\rm m}06.8^{\rm s}$, $\delta_{1950.0} = +13°29'42''$) is a standard phase calibrator at OVRO. The line of sight to it crosses the outer edge of the dark cloud B30, part of the λ Ori ring of clouds (Maddalena & Morris 1987), 1.5° ($\sim$ 10 pc) north of the bright rim compressed by the S264 H II region. Here the gas is probably as yet unperturbed by the hot expanding gas of S264.

The observations of 0528+134 used in this Letter were obtained between September 1993 and May 1994 with a typical spatial resolution of 5″. Phase calibration was obtained by self–calibration, and fluxes of 5 Jy at 3 mm and 2.5 Jy at 1.3 mm were assumed. The derived optical depths and the subsequent analysis are independent of the assumed flux. The shape of the passband was flattened by dividing by a polynomial fit of third order or less to the average spectrum of 3C273 or 3C454.3. This procedure resulted in very flat baselines; the Galactic emission and absorption found toward 3C454.3 (Liszt & Wilson 1993, de Geus & Phillips 1995) does not fall in the $V_{\rm LSR}$ range of the spectra. The spectral resolution ranges from 0.10 to 0.35 $\rm km\,s^{-1}$. It is assumed that the extended emission is completely resolved out by the interferometer.

Detection of ^{12}CO 1–0 emission has been reported by Liszt & Wilson (1993) using NRAO 12m telescope (beam size 60″). Moore et al. (1994) report the observation of H_2CO

$1_{10} - 1_{11}$ absorption with the VLA.

3. Results

The observed spectra are presented in Fig. 1. Parameters of Gaussian profile fits to the observed spectra are given in Tab. 1. The absorption lines of ^{12}CO, HCO$^+$, and HCN occur at $V_{\rm LSR} = 9.5 \pm 0.1$ km s^{-1}. Only two of the three hyperfine components of HCN fall completely in the passband, the third lies at the edge. No absorption has been detected of ^{13}CO 1–0 and CS 2–1. The ^{12}CO 1–0 absorption line with FWHM 0.76 km s^{-1} is only marginally resolved at the resolution of 0.35 km s^{-1}, but is consistent with the fully resolved emission profile of 0.80 km s^{-1} FWHM (Liszt & Wilson 1993). The HCO$^+$ 1–0 spectrum shows a second, shallow absorption feature at $V_{\rm LSR} = 2.1$ km s^{-1}. No counterpart is present in ^{12}CO 1–0 absorption nor in emission at this position, but emission at this $V_{\rm LSR}$ is found $2'$ south (Liszt & Wilson 1993).

Although similar opacities are derived for ^{12}CO and HCO$^+$, significantly different line widths of 0.76 and 1.30 km s^{-1} FWHM are found at the respective resolutions of 0.35 km s^{-1} and 0.42 km s^{-1}. Contaminating CO emission in the interferometer beam would only aggravate the discrepancy. The main line of HCN has a width of 1.1 km s^{-1} (resolution 0.21 km s^{-1}) but an opacity of only 0.44. Therefore the observed differences in line width cannot be attributed to line saturation. In §4 an explanation in terms of turbulence and cloud chemistry is proposed.

An escape probability code has been used to derive the H$_2$ number density $n_{\rm H_2}$, the kinetic temperature $T_{\rm kin}$, and the molecular column densities, including collisions with H$_2$ and electrons. Details of the code and references to the adopted cross sections can be found in Jansen, van Dishoeck & Black (1994). It is assumed that all hydrogen is in molecular form. An electron fraction $x_{\rm e} = n_{\rm e}/n_{\rm H_2} = 5 \times 10^{-5}$ has been assumed, which is expected to be a reasonable average of the variation of x_e with depth into a translucent cloud (Gredel et al. 1994). From the observed ^{12}CO emission and absorption, the density is constrained to $n_{H_2} = 100 - 500$ cm^{-3}, and the ^{12}CO column density to $N = (1.5 - 5.0) \times 10^{15}$ cm^{-2}, assuming that the physical characteristics in the $5''$ and $60''$ beams are equal (see Fig. 2). The ^{12}CO 1–0 antenna temperature from Liszt & Wilson (1993) has been corrected for main beam efficiency only. Because of its small dipole moment, electron collisions are unimportant for CO. Since the $J = 1$ and $J = 2$ levels are located at 5.5 K and 16.6 K above the ground level respectively, the kinetic temperature has no great influence on the excitation. The observed ^{12}CO 2–1 optical depth constrains the kinetic temperature to $\gtrsim 20$ K. The inferred density of a few hundred cm^{-3} is typical for translucent clouds (van Dishoeck & Black 1989) and is an order of magnitude lower than that inferred for the lines of sight studied by Lucas & Liszt (1994).

HCO^+, HCN and CS have much larger dipole moments than CO, but the inferred n_{H_2} is two or three orders smaller than the critical density of the observed transitions. Their excitation is therefore dominated by the cosmic background radiation field, and hence the derived column densities are largely insensitive to variations in x_e. Only for H_2CO does the uncertainty in x_e prohibit an accurate determination of the column density. In Tab. 1 the inferred column densities and upper limits are listed. The predicted corresponding antenna temperatures for HCO^+ and HCN emission are ~ 0.03 K and ~ 0.01 K respectively.

4. Discussion

In dark clouds like TMC–1 abundances of $HCO^+/^{12}CO$ and $HCN/^{12}CO$ of $(1-3) \times 10^{-4}$ are found. It is therefore remarkable that in this translucent, low density cloud values as high as $(2.5 - 14.0) \times 10^{-4}$ and $(3.6 - 16.0) \times 10^{-4}$ respectively are inferred. For other lines of sight Lucas & Liszt (1994) reach similar conclusions. For the velocity component at

$V_{\rm LSR} = 2.1$ km s^{-1} an even larger value of HCO$^+$/CO$> 5 \times 10^{-3}$ is found assuming similar conditions as for the 9.5 km s^{-1} component. Although such large abundance ratios could be partially due to a low CO abundance because a large fraction of carbon is atomic, the absolute column densities of HCO$^+$ and HCN are much higher than can be explained by current chemical models.

Chemical models are constrained by the number density of hydrogen nuclei $n = n_{\rm H} + 2n_{\rm H_2}$, the gas kinetic temperature $T_{\rm kin}$, the H_2 column density $N_{\rm H_2}$, the intensity of the incident ultraviolet radiation field $I_{\rm UV}$, and the elemental depletions. Assuming that all hydrogen is molecular, n is found from the ^{12}CO excitation. An H_2 column density of $(1.0 \pm 0.5) \times 10^{21}$ cm^{-2} is adopted based on the observed integrated CO emission with the conversion factor of Bloemen (1989), and on the 100 μm IRAS flux (de Vries & le Poole 1985) and the $A_{\rm v}/N$ conversion of Savage et al. (1977). The incident radiation field is assumed to be enhanced by a factor of 2 with respect to the average interstellar radiation field, $I_{\rm UV} = 2$, which is not implausible given the vicinity of the λ Ori association. The elemental depletions found toward ζ Oph are adopted (Cardelli et al. 1993; Savage, Cardelli & Sofia 1992).

It is proposed that cloud turbulence can explain both the observed high abundances and the line widths of HCO$^+$ and HCN (Spaans, Black & van Dishoeck 1995). In the first part of Tab. 2 the results of chemical modeling without turbulence are presented for a number of molecules, using $n = 250$ cm^{-3}, $T_{\rm kin} = 60$ K, $N_{\rm H_2} = 1.0 \times 10^{21}$ cm^{-2}, and $I_{\rm UV} = 2$. For these parameters the model clearly fails to produce the observed amounts of HCO$^+$ and HCN by two orders of magnitude. Even for the highest density consistent with the observations, $n = 10^3$ cm^{-3}, the produced column densities of HCO$^+$ and HCN are not significantly increased.

The second part of Tab. 2 gives the results for chemical modeling including the effects of turbulence for the same cloud parameters. A turbulent velocity structure differs from a pure Gaussian shape by excess power in the line wings, as has been observed toward dark clouds (Falgarone & Phillips 1990). Spaans et al. (1995) discuss the possible formation of the observed large amounts of CH^+ in diffuse clouds in general through the endothermic reaction $C^+ + H_2 \rightarrow CH^+ + H$, where turbulence provides the translational energy needed to overcome the reaction barrier. A relatively high fraction of CH^+ is produced with a large velocity dispersion. Since CH^+ is rapidly converted to CH_2^+ it cannot thermalize by elastic collisions with H_2, explaining its observed broad line profiles. It is proposed here that any species whose formation involves CH^+ will inherit part of this broad velocity distribution provided that both the formation and the destruction proceed on time scales shorter than needed for thermalization. Both the formation of HCO^+ and HCN involves CH^+ through the reactions $CH^+ + O \rightarrow CO^+ + H$; $CO^+ + H_2 \rightarrow HCO^+ + H$ and $CH_2^+ + N \rightarrow HCN^+$; $HCN^+ + H_2 \rightarrow H_2CN^+ + H$; $H_2CN^+ + e \rightarrow HCN + H$. Spaans et al. (1995) present the results of a parameter study of the effects of turbulence on the chemistry. The critical input parameter is $\Delta V_{\rm turb}$, a measure of the total kinetic energy per unit mass injected into the medium on the largest scales. Resulting line profile widths are calculated by making simple assumptions about the redistribution of translational energy by the subsequent reactions, and by assuming a FWHM of 0.80 km s^{-1} for the 'quiescent' gas. For $\Delta V_{\rm turb} = 3.5$ km s^{-1}, the resulting line widths are $\Delta V(HCO^+) = 1.5$ km s^{-1}, $\Delta V(HCN) = 1.1$ km s^{-1} and $\Delta V(^{12}CO) = 0.9$ km s^{-1}, convolved with the respective instrumental resolutions (§3). It can be seen that this model explains the observed line widths and column densities reasonably well for the derived parameters. In particular, HCO^+ and HCN are enhanced by two orders of magnitude, and even CO is increased by a factor of four. Note that the enhanced CO abundance also leads to additional HCO^+ through the $CO + H_3^+$ reaction. Although the details depend sensitively on the adopted parameters, the computed trends are robust. Only for H_2CO are the predicted column densities too low by several orders of magnitude, but grain surface reactions, which could be important, have not been included. The adopted value of $\Delta V_{\rm turb}$ is a factor of 2 larger than the values inferred by Gredel et al. (1994) for high latitude clouds, which is not unexpected since the compression of B30 on one side by the expanding hot gas of S264 deposits large amounts of energy in the cloud.

We conclude that in this low density, diffuse cloud, the turbulence influences the cloud chemistry dramatically, as reflected in the high HCO^+ and HCN abundances and their line profiles. For densities $n > 10^3$ cm^{-3} the CH^+ formation is strongly suppressed, since the mean free path on which C^+ reacts with H_2 to form CH^+ becomes less than the scale length on which the turbulence is dissipated. It is therefore only in low density clouds such as this one that the effects of turbulence on the chemistry become apparent. Liszt & Lucas (1994) report similar column densities of ^{12}CO and HCO^+ toward ζ Oph, a line of sight of similar physical conditions. The measured CH^+ column density toward ζ Oph is of the same order of magnitude as predicted for our line of sight. The observations presented by Lucas & Liszt (1994) show velocity components with very broad HCO^+ and HCN profiles in the absence of ^{12}CO emission, suggesting very low densities. This shows that searches for molecular absorption should not be limited to lines of sight with detected CO emission. Because of its high dipole moment and relatively large abundance, HCO^+ absorption line studies sample regions which cannot be observed in molecular emission or even in CO absorption.

This work was supported by a PIONIER grant of the Netherlands Organization for Scientific Research (NWO). The Owens Valley Millimeter Array is operated under funding from NSF grant AST 93-14079, which also supports EdG. The authors thank A. Marscher for communicating the H_2CO results before publication and providing valuable comments on the manuscript, and J.H. Black and H.S. Liszt for useful discussions.

Table 1: Absorption line parameters and inferred column densities

Species	$V_{\rm LSR}$ (km s^{-1})	ΔV (km s^{-1})	τ	N [a] (cm^{-2})	$N/N_{\rm CO}$
^{12}CO 1–0	9.40	0.76	1.33 ± 0.20	$(1.5 - 6.0) \times 10^{15}$	$\equiv 1$
^{12}CO 2–1	9.60	0.92	$1.37^{+1.56}_{-0.58}$	...	...
^{13}CO 1–0	...	...	< 0.05	$< 4.0 \times 10^{14}$	< 0.26
HCO$^+$ 1–0	9.53	1.30	1.49 ± 0.08	$(2.3 \pm 0.1) \times 10^{12}$	$(3.6 - 16.0) \times 10^{-4}$
	2.10	2.8	0.08 ± 0.01	$(2.6 \pm 0.1) \times 10^{11}$	$> 5.0 \times 10^{-3}$
HCN 1,2–0,1	9.61	1.06	0.44 ± 0.07	$(1.8 \pm 0.3) \times 10^{12}$	$(3.5 - 14.0) \times 10^{-4}$
1,1–0,1		1.26	0.24 ± 0.07		
1,0–0,1		0.84	0.10 ± 0.05		
CS 2–1	...	...	< 0.13	$< 1.0 \times 10^{12}$	$< 6.7 \times 10^{-4}$
H$_2$CO $1_{10} - 1_{11}$	9.5	...	0.021 ± 0.007	$> 6.0 \times 10^{12}$ [b]	$> 1 \times 10^{-4}$

[a] Column densities derived using $n_{\rm H_2} = 100 - 500$ cm^{-3}, $T_{\rm kin} = 20 - 60$ K, $x_{\rm e} = 5 \times 10^{-5}$.

[b] Lower limit neglecting electron collisions.

Table 2: Results of 'quiescent' and turbulent chemical models

Species	N (cm^{-2})	
	$\Delta V_{\rm turb} = 0$	$\Delta V_{\rm turb} = 3.5$ km s^{-1}
^{12}CO	5.5×10^{14}	2.1×10^{15}
^{13}CO	4.7×10^{13}	6.6×10^{13}
CH$^+$	2.2×10^{11}	5.1×10^{13}
CH	3.2×10^{13}	9.5×10^{13}
C$_2$H	3.5×10^{13}	9.6×10^{13}
HCO$^+$	8.2×10^{9}	6.2×10^{11}
HCN	7.2×10^{9}	9.3×10^{11}
CS	1.2×10^{10}	1.9×10^{11}
CN	1.1×10^{13}	3.9×10^{13}
H$_2$CO	1.4×10^{8}	2.4×10^{8}

REFERENCES

Bania, T. M., Marscher, A. P., & Barvainis, R. 1991, AJ 101, 2147

Bloemen, J. B. G. M. 1989, ARA&A 27, 469

Cardelli, J. A., Mathis, J. S., Ebbets, D. C., & Savage, B. D. 1993, ApJ 402, L17

Colgan, S. W. J., Salpeter, E. E., & Terzian, Y. 1986, AJ 91, 107

Cox, P., Güsten, R., & Henkel, C. 1988, A&A 206, 108

Crawford, I. A., Barlow, M. J., Diego, F., & Spyromylio, J. 1994, MNRAS 266, 903

Crutcher, R. M. 1980, ApJ 239, 549

de Geus, E. J., & Phillips, J. A. 1995, in preparation

de Vries, C. P., & le Poole, R. S. 1985, A&A 145, L7

Falgarone, E., & Phillips, T. G. 1990, ApJ 459, 344

Jansen, D. J., van Dishoeck, E. F., & Black, J. H. 1994, A&A 282, 605

Gredel, R., van Dishoeck, E. F., & Black, J. H. 1993, A&A 269, 477

Gredel, R., van Dishoeck, E. F., & Black, J. H. 1994, A&A 285, 300

Lequeux, J., Allen, R. J., & Guilloteau, S. 1994, A&A 280, L23

Liszt, H. S., & Wilson, R. W. 1993, ApJ 403, 663

Liszt, H. S., & Lucas, R. 1994, ApJ 431, L131

Lucas, R., & Liszt, H. S. 1994, A&A 282, L5

Maddalena, R. J., & Morris, M. 1987, ApJ 323, 179

Marscher, A. P., Bania, T. M., & Wang, Z. 1991, ApJ 371, L77

Moore et al. 1994, in preparation

Savage, B. D., Bohlin, R. C., Drake, J. F., & Budich, W. 1977, ApJ 216, 291

Savage, B. D., Cardelli, J. A., & Sofia, U. J. 1992, ApJ 401, 706

Spaans, M., Black, J. H., & van Dishoeck, E. F. 1995, ApJ submitted

Scoville, N. Z., Carlstrom, J. E., Chandler, C. J., Phillips, J. A., Scott, S. L., Tilanus, R. P. J., & Wang, Z., 1993. PASP 105, 1482

van Dishoeck, E. F., & Black, J. H. 1989, ApJ 340, 273

Wilson, T. L., & Mauersberger, R. 1994, A&A 282, L41

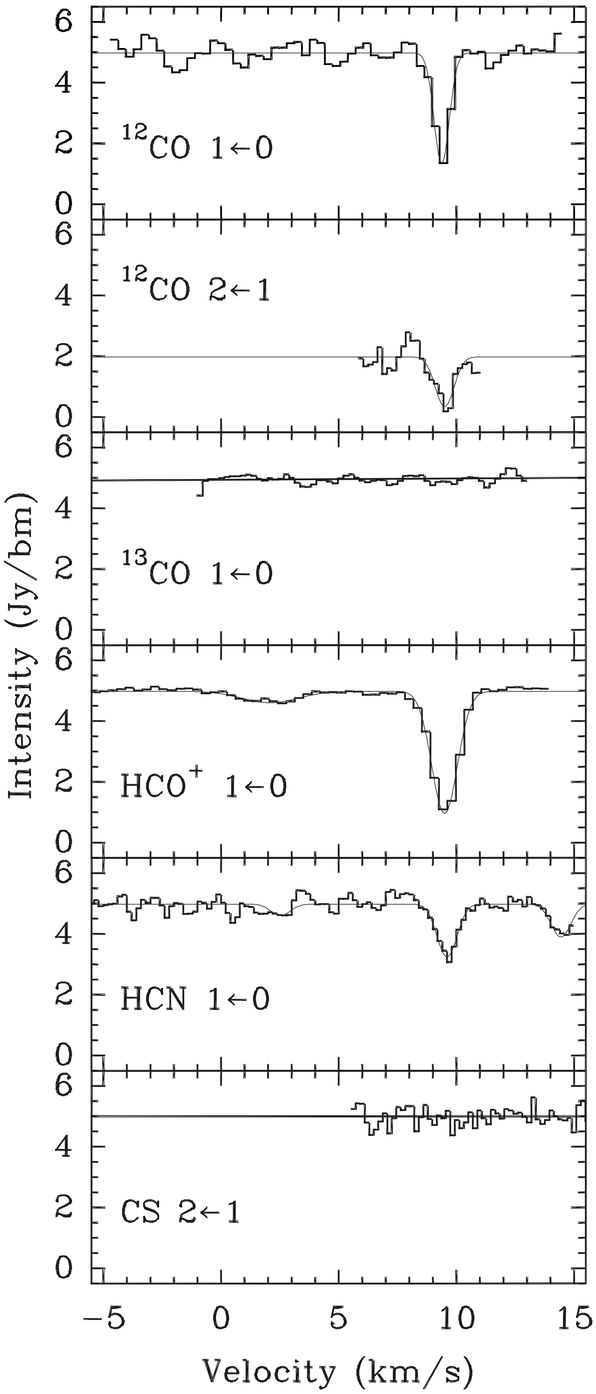

Fig. 1.— Spectra obtained toward PKS 0528+134 with the Owens Valley Millimeter Array. Horizontal scale is $V_{\rm LSR}$ in km s^{-1}, vertical scale is intensity in Jy per beam

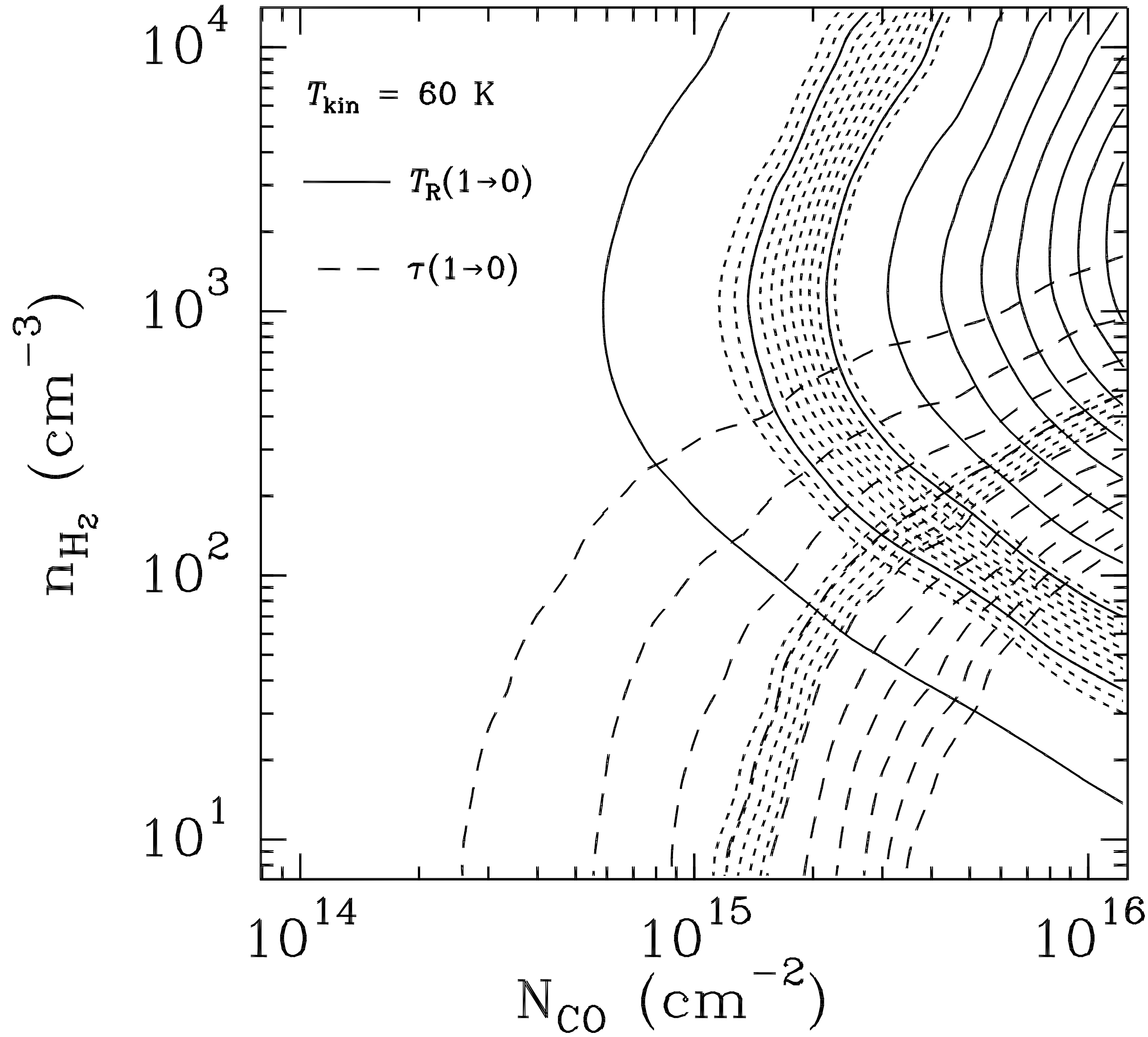

Fig. 2.— Contour plots of ^{12}CO 1–0 emission (solid line) and line center optical depth (dashed line) as function of ^{12}CO column density and H_2 number density for $T_{\rm kin} = 60$ K. Contour levels are $T_{\rm R} = 1.0,\ 2.0\ldots$ K, and $\tau = 0.3,\ 0.6\ldots 3.0$. Observed values are indicated with their respective accuracies. For the lowest temperature consistent with the observations, $T_{\rm kin} = 20$ K, the inferred $n_{\rm H_2}$ is only enhanced by about a factor two